Metallomics

Accepted Manuscript

This article can be cited before page numbers have been issued, to do this please use: M. Nisavic, G. V. Janji, A. Hozic, M. Petkovi, M. Milcic, Z. Vujcic and M. Cindric, *Metallomics*, 2018, DOI: 10.1039/C7MT00330G.

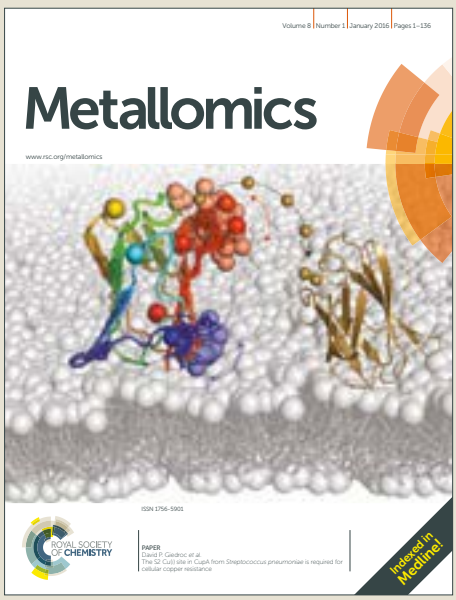

ROYAL SOCIETY OF CHEMISTRY

rsc.li/metallomics

View Article Online
DOI: 10.1039/C7MT00330G

Journal Name

ARTICLE

Positive and negative nano-electrospray mass spectrometry of ruthenated serum albumin supported by docking studies: an integrated approach towards defining metallodrug binding sites on proteins

Received 00th January 20xx,
Accepted 00th January 20xx

DOI: 10.1039/x0xx00000x

www.rsc.org/

Marija Nišavić[a], Goran V. Janjić[b], Amela Hozić[c], Marijana Petković[a], Miloš K. Milčić[d], Zoran Vujčić[d] and Mario Cindrić[c]*

Binding of three ruthenium(II) compounds of general formula *mer*-[Ru(L3)(*N*-*N*)X][Y] (where L3 = 4'-chloro-2,2':6',2''-terpyridine (Cl-tpy); *N*-*N* = 1,2-diaminoethane (*en*), 1,2-diaminocyclohexane (*dach*) or 2,2'-bipyridine (*bipy*); X = Cl; Y = Cl) to human serum albumin (HSA) has been investigated by nano-LC/nano-ESI MS and docking studies. *Bottom-up* proteomics approach has been applied for structural characterization of metallated protein and the data were analyzed in both, positive and negative ion mode. The negative ion mode has been achieved after post-column addition of isopropanol solution of formaldehyde that enabled sample ionization under micro-flow rates. Negative ion mode MS have proved to be beneficial for the analysis of binding sites on ruthenated protein in terms of ion charge reduction and consequent simplification of target sequence identification based on isotopic differences between ruthenated and non-ruthenated peptides. Moreover, negative ion mode ESI MS shows the advantage of singly charged ion formation and, unlike MALDI MS, does not cause complete ligand fragmentation, merging the benefits of each method into a single experiment. Six target sequences were identified for the binding of *en* and *dach* compounds, and four sequences for the binding of *bipy*. All compounds have been found to bind histidine and one aspartate residue. Docking studies showed that the identified sequences are constituents of five distinct binding sites for *en* and *dach*, or two sites for *bipy* complex. The selection of binding sites seems to be dependent on chelate ligand and on form of the complex prior or after hydrolysis of leaving chloride ligand.

Significance to metallomics

Improving mass spectrometry-based analytical methodology for structural characterization of metallodrug-protein interaction has become an important goal in the field of bioinorganic chemistry. Here, we introduce negative ion mode nano-LC/nano-ESI MS as a tool for determination of binding sites of three Ru(II) compounds on human serum albumin. Complemented with positive ion mode and docking studies, MS$^-$ analysis showed distinct advantages over existing methodology. The results revealed effects of chelate and leaving ligands on binding site selection.

Introduction

Low selectivity, severe toxicity and acquired resistance of platinum drugs prompted the development of novel metal-based chemotherapeutics. Ruthenium compounds have emerged as promising candidates due to their low toxicity, increased selectivity towards cancer cells and pronounced antimetastatic effect[1–3]. Consequent growing interest in ruthenium-based compounds has shifted the spotlight from DNA to proteins as potential biomolecular targets responsible for anticancer activity of these drugs[4].

Mass spectrometry (MS) has drawn considerable interest as a tool for structural characterization of metallodrug-protein interactions due to its accuracy, short analysis time and low sample consumption[5,6]. Further, transition metals such as Pt or Ru have distinct isotopic distributions that are not naturally encountered in biological samples, which facilitates targeted analysis and justifies the choice of MS methods for this application. Among soft ionization MS techniques, matrix-assisted laser desorption ionization (MALDI) and electrospray ionization (ESI) are most often employed for characterization of metallodrug-protein interactions. Although singly charged ion formation is a significant advantage of MALDI MS in terms of facile identification of metallated peptides based on isotopic differences, it is not so commonly used due to *in-source* fragmentation of coordinated metal compounds[7].

[a]Department of Physical Chemistry, "Vinča" Institute of Nuclear Sciences, University of Belgrade, Mike Petrovića Alasa 12-14, 11000 Belgrade, Serbia
[b]Institute of Chemistry, Technology and Metallurgy, University of Belgrade, Njegoseva 12, 11000 Belgrade, Serbia
[c]Centre for Proteomics and Mass Spectrometry, Division of Molecular Medicine, Ruđer Bošković Institute, Bijenička cesta 54, 10000 Zagreb, Croatia
[d]Faculty of Chemistry, University of Belgrade, Studentski trg 12-14, 11000 Belgrade, Serbia
*** Correspondence to: mcindric@irb.hr**
Electronic Supplementary Information (ESI) available: Full experimental details and additional results referenced within the text. See DOI: 10.1039/x0xx00000x

View Article Online
DOI: 10.1039/C7MT00330G

Electrospray ionization proved to be more suitable for this purpose because the protein-bound compounds largely remain intact during the process of ionization[7]. Further, the ease of hyphenation of ESI MS to liquid chromatography (LC) and other separation techniques, makes it more convenient for direct analysis of peptides in a typical *bottom-up* proteomics approach. The main disadvantage of ESI is multiple charging that can aggravate identification of metallated peptides because it is challenging to differentiate between isotopic distributions of modified and larger non-modified peptides. Further, multiple charge state distributions can lead to isobaric interferences and mass spectral congestion in complex samples. Consequently, ESI MS-based data describing metallodrugs' binding sites on larger, biologically relevant proteins and cellular targets is scarce[8,9].

In this work, we have used nano-LC/nano-ESI MS for determination of binding sequences and target amino acids for the binding of three ruthenium compounds of general formula *mer*-[Ru(L3)(*N*-*N*)X][Y] (where L3 = 4'-chloro-2,2':6',2''-terpyridine(Cl-tpy); *N*-*N* = 1,2-diaminoethane (en), 1,2-diaminocyclohexane (dach) or 2,2'-bipyridine (bipy); X = Cl; Y = Cl)[10] (Fig. 1), to human serum albumin (HSA). The selected highly water-soluble Ru compounds proved to be moderately cytotoxic towards several cancer cell lines and showed strong binding to both, DNA and proteins[10,11]. Human serum albumin is the main protein responsible for drug transport and uptake, but is also considered to be the key for anticancer activity of several Ru drug candidates. Clinically relevant KP1019 and its sodium salt analogue NKP-1339 are believed to exhibit tumor selectivity trough HSA-mediated pathway that is based on enhanced permeability and retention (EPR) effect of tumor tissues[12]. The EPR effect is attributed to defective architecture of tumor blood vessels that allows macromolecules (>40 kDa) such as HSA-drug complex to transit trough gaps in endothelial cells of blood vessels and accumulate in tumor tissue[13].

Fig. 1. Structural formula of $[Ru(Cl\text{-}tpy)(en)Cl]^+$ (**1**), $[Ru(Cl\text{-}tpy)(dach)Cl]^+$ (**2**) and $[Ru(Cl\text{-}tpy)(bipy)Cl]^+$ (**3**).

So far, MS-based analysis of metallodrug binding to proteins has been performed almost exclusively in the positive ion mode, while the negative ion mode has been rarely applied.[14,15] This study describes identification of HSA binding sites for selected Ru compounds in both, positive and negative ion modes and discusses the advantages of each approach, as well as their complementarity and suitability for wider applications. Further, docking studies have been used to complement and rationalize the obtained experimental data.

Experimental

General procedures

Angiotensin II and HSA, purchased from Sigma-Aldrich (St. Louis, MO, USA), were dissolved in 25 mM sodium bicarbonate buffer of pH 7.8 to a concentration of 1 mg/mL. Angiotensin II was mixed with 5 µL of each complex solution, obtained after dissolving a small amount of $[Ru(4'\text{-}Cl\text{-}tpy)(en)Cl]^+$ (**1**), $[Ru(4'\text{-}Cl\text{-}tpy)(dach)Cl]^+$ (**2**) and $[Ru(4'\text{-}Cl\text{-}tpy)(bipy)Cl]^+$ (**3**)[10,11] in miliQ water, and diluted to a final concentration of 0.1 mg/mL. After 3h of incubation at 37° C, each Ru-bound peptide was purified using ZipTip C18 column (Eppendorf, Hamburg, Germany). Human serum albumin was mixed with each Ru compound in 1:10 molar ratio, diluted to 0.1 mg/mL concentration and incubated for 24 h at 37° C. After the incubation, unbound complexes were removed upon extensive ultrafiltration using Centricon ultrafiltration units (10 kDa cut off; Millipore Co.). The remaining HSA-Ru adducts were diluted to a starting concentration and subjected to trypsin (Merck, Germany) digestion (5 µL of 1 mg/mL trypsin) at 37° C for 18 h. Both, angiotensin and HSA tryptic digest were dried in centrifugal vacuum evaporator (Eppendorf) and resuspended in 0.1% formic acid (Kemika, Zagreb, Croatia) to a 0.1 mg/mL concentration prior to MS measurements. Acetonitrile used for LC mobile phase preparation, formaldehyde and isopropanol used for negative ion mode enhancement, as well as leucine enkephaline used as a reference material for MS calibration were all purchased from Sigma-Aldrich.

LC/MS conditions

The obtained HSA peptides were resolved on nanoACQUITY UPLC (Waters, Milford, MA, USA), equipped with nanoACQUITY UPLC 2G-V/M Symmetry C18 Trap Column (100Å, 5µm, 180 µm x 20 mm) and ACQUITY UPLC BEH130 C18 Analytical Column (130 Å, 1.7 µm, 100 µm × 100 mm). The injection volume was 4 µL and column temperature 40° C. Isocratic delivery of mobile phase A (0.1 % formic acid) to the trap column was performed at 15 µL/min for 2 min. Elution of the peptides was performed using a gradient of mobile phase B (0.1% formic acid in 95% acetonitrile) from 0.1% to 99% in 30 min, at 1 µL/min flow rate. Mass spectrometry measurements were performed on SYNAPT G2-Si mass spectrometer (Waters, Milford, MA, USA). Capillary and cone voltages were set to 3.5 kV and 40V, respectively. Source temperature was 80° C and nanoflow gas pressure 1 bar. Post-column addition of 0.1% formaldehyde in isopropanol was performed at a flow rate of 0.4 µL/min. The data was recorded in positive and negative MS^E resolution mode[16,17], covering a mass range between 50 and 4000 Da. Collision cell energy was alternating between low energy (4 eV) to collect peptide precursor (MS) data, and elevated energy (ramping from 20 to 40 eV) to obtain peptide fragmentation (MS^E) data. The lock spray (1 ng/µL leucine enkephalin in 50:50 IPA/0.1% formic acid) was introduced every 1 min to ensure high mass accuracy.

The positive ion mode data was processed using PLGS software (PLGS; v 3.0.1, Waters). Database containing HSA sequence was created and the data were searched with trypsin as a digestion reagent, with two potential miscleavages. Peptide and fragment tolerance were set to automatic. Apart from oxidation M and dehydration ST, monoisotopic mass of each $[Ru(Cl\text{-}tpy)(\textit{chel})]^{2+}$ complex was set as variable side chain modification in corresponding data set. Two mass units were substracted from each complex mass, to compensate for twofold charge of the complexes.

MALDI MS/MS measurements were performed as described previously[11].

Computational studies

View Article Online
DOI: 10.1039/C7MT00330G

The full geometry optimization of all ruthenium complexes were carried out with B3LYP hybrid functional using 6-31g** basis set for all non metal atoms and standard lanl2dz basis set for ruthenium atom (with effective core potential (ECP) for inner electrons). The harmonic vibrational frequencies were evaluated for each fully optimized structure at same level of theory to confirm the nature of the found minima and no imaginary frequencies were found. All quantum chemical calculations, needed to determine the equilibrium constants, were carried out using the GAUSSIAN09 program package[18].

Crystal structures of human serum albumin (HSA, PDB code 1BM0[19]) for docking study was extracted from a Protein Data Bank[20]. The water molecules and all other ligand residues were removed from the structure. Optimized structures of metal complexes and structure of HSA protein were used for doking preparation in AutoDockTools program, while the docking study was done with AutoDock program[21]. All protein residues were kept rigid and all single ligand bonds were set to be rotational. A grid box, containing the whole protein, was used to accommodate the ligand to move freely during docking run.

Results and discussion

Binding of the complexes to angiotensin II

In order to investigate the behavior of peptide-bound ruthenium compounds in positive and negative ESI mode, MS spectra were first recorded after the incubation of each compound with a model peptide, angiotensin II (Fig. S1). In the positive ion mode, formed ruthenated angiotensin is detected as a triply-charged ion in case of all three compounds. Upon Cl ligand hydrolysis and subsequent complex binding, the peptide is provided with extra positive charge originating from metal center and multiple charging is therefore favored. Negative ion mode spectra (Fig. S2) are acquired after post-column addition of formaldehyde dissolved in isopropanol, as a negative ion mode modifier. The application of negative ion mode modifiers, their mechanism of action and advantages of their use in nano-ESI MS analysis of peptides have been explained thoroughly in our recent paper[22]. The predominant species detected in all negative ion mode MS spectra are singly charged ions of ruthenated angiotensin, as well as their formic acid adducts. This can be explained with analytes' intrinsic positive charge that prevents multiple charging in the negative ion mode. This approach can be observed as a way of ion charge reduction that accounts for significant method simplification. More precisely, the produced effect implies the obtaining of *MALDI-like* ESI MS spectra. In this way, the advantages of MALDI singly charged ion formation and ESI preservance of intact metallodrug-peptide/protein interactions are merged in a single experiment.

Binding of the complexes to human serum albumin

Positive ion mode

In order to optimize nano-ESI MS-based approach for facilitated target sequence identification, MS^E data were recorded in positive ion mode for each Ru compound-HSA tryptic digest resolved on reversed-phase nano-UPLC column. The above mentioned challenges of manual identification of target sequences for binding of ruthenium have been addressed by setting each complex mass (without leaving Cl ligand) as an amino acid side chain modification and processing the obtained data using ProteinLynx Global Server (PLGS) software. Since MS^E data includes low energy (LE) and high energy (HE) spectra of the analyzed samples, both, target sequences and target amino acids for each Ru compound could be identified from a single dataset. The identified target sequences are shown in LE MS^E spectra (Fig. S3, S4 and S5 for compound **1**, **2** and **3**, respectively).

For compound **1** and **2** six target sequences were found (five using PLGS and one manually), while compound **3** showed lower binding affinity towards the protein with four target sequences detected. This is probably because, unlike *en* and *dach*, *bipy* ligand lacks the ability of strong hydrogen bond formation with the surrounding amino acid residues. Target amino acid residues were determined based on HE MS^E spectra. The compounds **1** and **2** target four histidine (His) and one aspartate (Asp) residues, while compound **3** targets two His and one Asp residues. An example of PLGS extracted HE MS^E spectrum for the binding of **1** to His of ^{146}HPYFYAPELLFFAK^{159} HSA sequence is shown in Fig. S6. The list of all software identified fragment ions for the target sequences of the selected compound **2** is shown in Table S1. The target amino acid of the remaining ^{1}DAHK^{4} sequence that was found manually will be discussed in the following section. We believe the herein described approach can also be used for identification of metallodrug target proteins in more complex samples, as previously described by Wills *et al* using a similar approach[23,24]. Further, the application of nano-LC/nano-ESI MS system has advantages in terms of low sample consumption and increased sensitivity comparing to conventional ESI MS[25]. This can be of uttermost importance because relevant drug targets are often low abundance proteins and the amount of sample available for measurements is often limited. Nevertheless, precaution should be made when working with more complex samples and the obtained results should be checked for metal isotopic distribution of the obtained fragment ions, to minimise false positives[23,24]. Also, the fact that proteomics software packages do not take into account metal isotopic distribution should be considered, as omission can happen during data processing. Despite of the accentuated challenges, the described approach greatly facilitates binding sequences identification.

Negative ion mode

The ability of peptides and metallopeptides to ionize in the negative ion mode under micro- and nano-flow rates has been attributed to formaldehyde proton scavenging effect and electrospray stabilizing effect of isopropanol[22]. Post-column addition of formaldehyde does not affect chromatographic separation or positive ion mode ionization efficiency, so complementary set of data can be obtained without additional changes in instrumental setup except switched polarities. Therefore, obtaining comparable results in the negative ion mode would present a direct confirmation of the results obtained in the positive ion mode and *vice versa*. To achieve this, target sequences for the binding of the tested compounds were identified manually in the negative ion mode LE MS^E spectra (Figures S7, S8 and S9 for compounds **1**, **2** and **3**, respectively). The identification was facilitated thanks to reduced multiple charging

View Article Online
DOI: 10.1039/C7MT00330G

and consequent significant isotopic differences between ruthenated and non-ruthenated peptides. Although the intensity of negative ions as well as the quality of the spectra decreases comparing to the positive ion mode (particularly with increasing *m/z*), negative ion mode proved to be sufficient for qualitative analysis. Moreover, good complementarity with the positive ion mode data was obtained, *e.i.* the same six target sequences were identified using either approach. In order to illustrate similarity between negative ion mode ESI MS and positive ion mode MALDI MS analyses, the spectra of DAHK peptide adduct with compound **2** are shown in Fig. 2. It can be seen that the detected ions are singly charged using either approach. Observable differences include complete loss of bidentate chelate ligand during MALDI analysis, while the chelate predominantly remains coordinated to ruthenium moiety during ESI process. This accounts for significant advantage of ESI MS, since no additional method is required to demonstrate that the loss of ligands is not due to solution hydrolysis, but MALDI in-source fragmentation[11].

Fig 2. Negative ion mode ESI MS (upper trace) and positive ion mode MALDI MS spectra (bottom trace) of DAHK sequence upon binding of $[Ru(Cl\text{-}tpy)(dach)Cl]^+$ complex.

Since the identity of DAHK target sequence was proposed solely based on mass shift and isotopic distribution, no information about target amino acid was obtained. For that reason, tandem mass analysis was performed in negative ESI mode. The obtained spectrum is compared to MALDI MS/MS spectrum in positive ion mode (Fig. 3). Unlike MS, MS/MS analysis in negative ESI mode leads to bidentate ligand fragmentation, as noted during MALDI analysis. All detected fragment ions in both spectra are singly charged, but they differ in between. It can be noted that mostly y-series ions are formed during ESI analysis while MALDI predominantly produces a and b ion series. The presence of ruthenated y_2 and x_2 ions in ESI, or b_3 and a_3 ions in MALDI spectrum indicates the binding of the compound to His3. The observed fragmentation type differences point out methodological complementarity.

Fig 3. Negative ion mode ESI MS/MS (upper trace) and positive ion mode MALDI MS/MS (bottom trace) spectra of DAHK sequence adduct with compound $[Ru(Cl\text{-}tpy)(dach)Cl]^+$. *indicates $[Ru(Cl\text{-}tpy)]^{2+}$ fragment.

In this study, negative ion mode ESI MS was used as a tool for determination of metallodrug binding sites on proteins. Moreover, we believe the herein applied method for negative ionization enhancement can also be used for simultaneous detection of metallodrug binding in a mixture of biomolecules. Separation and simultaneous MS detection of adducts formed between metallodrug and oligonucleotide or protein has been recently shown using capillary zone electrophoresis coupled to ESI MS[26]. In this study, oligonucleotide metallation was resolved at a single nucleotide level. The spectra could be obtained only in the positive ion mode, because the negative charge of the nucleotide fragments is cancelled due to positive charge of the attached metal compound, which prevented negative ionization. Here, we have shown that, under the same operating conditions (except switched polarities), negative ionization of metallated peptides can be achieved, despite intrinsic positive charge of the analyte. Therefore, we believe the same could apply for *e.g.* metallodrug-(oligo)nucleotide binding investigation, which accentuates the potential of the presented approach to be used for wider applications than presented herein.

Docking studies

In order to rationalize the experimentally obtained data, docking studies have been performed. The investigated complexes are known to bind proteins after Cl ligand exchange, followed by aquation and subsequent coordination to electron-donor amino acid residues[10,11]. Aquation rate proved to be dependent on the nature of chelate ligands in chloride containing complexes and is linked to drugs' cytotoxic effect[27]. Since blood chloride concentration is relatively high (104 mM), the hydrolysis is mostly supressed and the complexes are in their less reactive chloro form. Chloride concentration desreases in cytoplasm (23 mM) and nucleus (4 mM), which favors formation of more reactive aqua species[28]. Aqua species are easily deprotonated, leading to hydroxo species formation. Although the predominance of the named species depends on the location of the complex (or experimental conditions), all of them (chloro-, aqua- or hydroxo-) are present in solution and are, therefore, included in docking studies. Based on the obtained MS results and spatial localization of the identified target sequences, it can be concluded that there are three HSA regions for the binding of the tested Ru compounds (Fig. S10) and only one of them belongs to major HSA drug binding sites. The first one is located at domain I, in close proximity to ^{146}HPYFYAPELLFFAK^{159} sequence. The second one is located between subdomains IA and IIA, occupying the space between ^{1}DAHK^{4}, ^{5}SEVAHR^{10} and ^{65}SLHTLFGDK^{73} sequences. The third binding region is located at IIB subdomain, between ^{324}DVFLGMFLYEYAR^{336} and ^{146}HPDYSVVLLLR^{159} sequences. During data interpretation, previously determined average number of bound complex molecules per protein (seven for compound **1**, nine for **2** and two for complex **3**) was taken into account[29]. The illustration of binding sites for each complex chloro-, aqua- and hydroxo- form is shown in Fig. S11 , while their respective binding energies are listed in Table S3. The obtained values indicate that chloro- complexes bind somewhat stronger when compared to hydroxo- species. Binding affinities are, in case of both, chloro- and hydroxo- complexes, highest in case of compound **2**, while compound **3** shows the lowest binding affinities. It is worth mentioning that AutoDock program has a standard deviation of about 2-3 kcal/mol for the free energy prediction[30], which is not sufficient to provide confident affinities of sites for binding of certain form of the complexes (in this case the tested solution is a mixture of chloro, aqua-, and hydroxo-form of complex **1**, **2**, or **3**), but some trend can be observed. As the chloro, aqua-, and hydroxo- forms do not bind to the same binding site on the protein, the exact values of binding energy are not necessary. The lowest number of binding sites was obtained for aqua species that were found to predominantely interact with surface amino acid residues. None of aqua complex binding sites correspond to MS-determined target sequences. By comparing all theoretically predicted binding sites with MS-obtained sequences, it can be concluded that there are five sites on HSA for binding of compounds **1** and **2**, and two sites for binding of

View Article Online
DOI: 10.1039/C7MT00330G

compound **3**. The location of the binding sites with respect to MS-identified sequences is shown in Fig. 4. , while their binding energies, MS-identified target amino acids and forms in which the complexes bind to each site are accentuated in Table S4.

Fig 4. HSA binding sites for $[Ru(Cl\text{-}tpy)(en)Cl]^+$ (**1**), $[Ru(Cl\text{-}tpy)(dach)Cl]^+$ (**2**) and $[Ru(Cl\text{-}tpy)(bipy)Cl]^+$ (**3**), obtained by docking studies. Chloro forms of the complexes are shown green, while hydroxo are red. MS-identified sequences are shown black.

According to the docking studies, all complexes show the highest affinity for the binding of the protein region located between IA and IIA subdomains, which includes ^{1}DAHK^{4}, ^{5}SEVAHR^{10} and ^{65}SLHTLFGDK^{73} sequences. There are two sites in this region for the binding of compounds **1** and **2**, and one site for the binding of **3.**
The ^{1}DAHK^{4} sequence that is one of the constituents of this binding site is known as a hallmark of albumin metal binding[31,32]. It comprises the N-terminal site (NTS) for binding of metals, mainly through coordination with His3 that is also found to be the target for the binding of **1**, **2** and **3**. About 2% of NTS of HSA is populated with Cu(II) and it makes HSA the second largest pool of cooper in human blood serum[32]. Another sequence that is a part of the second binding site in this protein region is ^{65}SLHTLFGDK^{73}. This sequence contains His67 whose imidazole nitrogen is a ligand for binding of various metals, and is described in literature as HSA metal binding site A[32]. Also, His67 together with His9 from ^{5}SEVAHR^{10} sequence has been identified as cisplatin binding site on HSA[33,34].

Table 1. Binding energies and target amino acids for coordination of investigated Ru(II) complexes **1**, **2** and **3** on HSA.

The binding region that encompasses ^{146}HPYFYAPELLFFAK^{159} sequence is located at the lower entrance to subdomain IB, consisted mainly of three α-helices that form hydrophobic groove. As shown by MS data, ruthenium center from each compound binds to imidazole nitrogen of His146. This amino acid has also been recently confirmed to be the target of KP1910, based on X-ray data[12].
The third binding region is located between IA and IIA subdomains and is consisted of ^{324}DVFLGMFLYEYAR^{336} i ^{338}HPDYSVVLLLR^{348} sequences. Compounds **1** and **2** both coordinate His338 and Asp324, while compound **3** only binds to Asp324. Monodentate binding of Ru compounds trough coordination of O atoms from Asp residues of various proteins have been reported before[35].
One interesting observation is that no Cys binding of the complexes has been identified. Human serum albumin contains one free Cys34 residue, that is often identified as a target for binding of various transition metal drugs[6]. Although binding of both, Ru(III) and Ru(II) drugs to Cys moiety has been reported[36–38], the ability of Ru complex to reach Cys34 of HSA seems to be ligand depended[39]. Namely, Cys34 residue is placed within a crevice of the protein that is not easily accessible to complexes that contain large ligands, due to steric hindrance. In the study describing Ru(II) arene compound binding to HSA, it has been demonstrated that *biphenyl* containing compound can not bind to Cys34, unlike *p-cymene* containing compound that is readily bound to Cys moiety[39]. Although expected as a potential target, Cys34 complex binding has not been identified in this study, due to the nature of large *Cl-tpy* ligand that prevents drug entrance into the protein crevice, as confirmed by docking studies (data not shown).

Conclusions

Here, we have described nano-LC/nano-ESI MS-based approach for identification of binding sites of three Ru coordination compounds of general formula [Ru(Cl-tpy)(chel)Cl]Cl on human serum albumin. This study introduces negative ion mode mass spectrometry as a tool for investigating interactions between transition metal compounds and proteins, with a potential for wider applications. Although positive ion mode MS^E approach enabled simultaneous, automatic identification of target sequences and target amino acids for the binding of the tested compounds, negative ion mode approach has shown distinct advantage of singly charged ion formation that significantly reduces the complexity of manual data interpretation. Performed analyses in both ion modes provide good reliability of the obtained data that includes six target HSA sequences for the binding of 1 and 2, and four sequences for the binding of compound 3. As shown by docking studies, the identified sequences are constituents of five distinct binding sites for 1 and 2, or two sites for compound 3. The choice of the binding site seems to be dependent on the form of the complex (chloro-, hydroxo- or aqua-). The strongest binding of the complexes were obtained for their chloro- form. Although Cl ligand hydrolysis suppression in blood is considered as a way of reduction of drugs' side reactivity, it is known that the largest portion of complexes end up bound to serum proteins[40] after intravenous administration and the obtained results offer an explanation. Finally, since identified target amino acid residues, His and Asp, are often implicated in catalytic processes, the obtained results also suggest the potential of the tested Ru compounds to alter catalytic activity of enzymes which could be relevant for their mode of action.

Conflicts of interest

There are no conflicts to declare.

Acknowledgements

This work was supported by the project ApliMetaFarma RC.2.2.08-0046, Ministry of Education, Science and Technological Development of the Republic of Serbia: (grant No. 172011) and STSM Grant from COST Action BM1403. Numerical simulations were run on the PARADOX supercomputing facility at the Scientific Computing Laboratory of the Institute of Physics Belgrade, supported in part by the Ministry of Education, Science and Technological Development of the RepFublic of Serbia.

Notes and references

1 P. Heffeter, M. Pongratz, E. Steiner, P. Chiba, M. A. Jakupec, L. Elbling, B. Marian, W. Körner, F. Sevelda, M. Micksche, B. K. Keppler and W. Berger, *J. Pharmacol. Exp. Ther.*, 2005, **312**, 281–289.
2 U. Jungwirth, C. R. Kowol, B. K. Keppler, C. G. Hartinger, W. Berger and P. Heffeter, *Antioxid. Redox Signal.*, 2011, **15**, 1085–1127.

View Article Online
DOI: 10.1039/C7MT00330G

3 R. Trondl, P. Heffeter, C. R. Kowol, M. A. Jakupec, W. Berger and B. K. Keppler, *Chem. Sci.*, 2014, **5**, 2925–2932.
4 I. Dragutan, V. Dragutan and A. Demonceau, *Molecules*, 2015, **20**, 17244–17274.
5 A. Casini, C. Gabbiani, E. Michelucci, G. Pieraccini, G. Moneti, P. J. Dyson and L. Messori, *J. Biol. Inorg. Chem. JBIC Publ. Soc. Biol. Inorg. Chem.*, 2009, **14**, 761–770.
6 M. Wenzel and A. Casini, *Coord. Chem. Rev.*, 2017, **352**, 432–460.
7 C. G. Hartinger, W. H. Ang, A. Casini, L. Messori, B. K. Keppler and P. J. Dyson, *J. Anal. At. Spectrom.*, 2007, **22**, 960–967.
8 C. G. Hartinger, M. Groessl, S. M. Meier, A. Casini and P. J. Dyson, *Chem. Soc. Rev.*, 2013, **42**, 6186–6199.
9 D. L. Wong and M. J. Stillman, *Chem. Commun. Camb. Engl.*, 2016, **52**, 5698–5701.
10 A. Rilak, I. Bratsos, E. Zangrando, J. Kljun, I. Turel, Ž. D. Bugarčić and E. Alessio, *Inorg. Chem.*, 2014, **53**, 6113–6126.
11 M. Nišavić, R. Masnikosa, A. Butorac, K. Perica, A. Rilak, L. Korićanac, A. Hozić, M. Petković and M. Cindrić, *J. Inorg. Biochem.*, 2016, **159**, 89–95.
12 A. Bijelic, S. Theiner, B. K. Keppler and A. Rompel, *J. Med. Chem.*, 2016, **59**, 5894–5903.
13 H. Maeda, J. Wu, T. Sawa, Y. Matsumura and K. Hori, *J. Control. Release Off. J. Control. Release Soc.*, 2000, **65**, 271–284.
14 D. L. Wong, A. Zhang, A. S. Faponle, S. P. de Visser and M. J. Stillman, *Metallomics*, 2017, **9**, 501–516.
15 A. Enriquez Garcia and F. Jalilehvand, *J. Biol. Inorg. Chem. JBIC Publ. Soc. Biol. Inorg. Chem.*, , DOI:10.1007/s00775-017-1524-6.
16 R. H. Bateman, R. Carruthers, J. B. Hoyes, C. Jones, J. I. Langridge, A. Millar and J. P. C. Vissers, *J. Am. Soc. Mass Spectrom.*, 2002, **13**, 792–803.
17 J. C. Silva, R. Denny, C. A. Dorschel, M. Gorenstein, I. J. Kass, G.-Z. Li, T. McKenna, M. J. Nold, K. Richardson, P. Young and S. Geromanos, *Anal. Chem.*, 2005, **77**, 2187–2200.
18 M. Frisch, G. Trucks, H. Schlegel, G. Scuseria, M. Robb, J. Cheeseman, G. Scalmani, V. Barone, B. Mennucci, G. Petersson, H. Nakatsuji, M. Caricato, X. Li, H. Hratchian, A. Izmaylov, J. Bloino, G. Zheng, J. Sonnenberg, M. Hada, M. Ehara, K. Toyota, R. Fukuda, J. Hasegawa, M. Ishida, T. Nakajima, Y. Honda, O. Kitao, H. Nakai, T. Vreven, J. Montgomery, J. Peralta, F. Ogliaro, M. Bearpark, J. Heyd, E. Brothers, K. Kudin, V. Staroverov, R. Kobayashi, J. Normand, K. Raghavachari, A. Rendell, J. Burant, S. Iyengar, J. Tomasi, M. Cossi, N. Rega, J. Millam, M. Klene, J. Knox, J. Cross, V. Bakken, C. Adamo, J. Jaramillo, R. Gomperts, R. Stratmann, O. Yazyev, A. Austin, R. Cammi, C. Pomelli, J. Ochterski, R. Martin, K. Morokuma, V. Zakrzewski, G. Voth, P. Salvador, J. Dannenberg, S. Dapprich, A. Daniels, Farkas, J. Foresman, J. Ortiz, J. Cioslowski and D. Fox, *Gaussian 09 Revis. B01 Gaussian Inc Wallingford CT*.
19 S. Sugio, A. Kashima, S. Mochizuki, M. Noda and K. Kobayashi, *Protein Eng.*, 1999, **12**, 439–446.
20 D. S. Goodsell, *RCSB Protein Data Bank*, , DOI:10.2210/rcsb_pdb/mom_2003_1.
21 G. M. Morris, D. S. Goodsell, R. Huey and A. J. Olson, *J. Comput. Aided Mol. Des.*, 1996, **10**, 293–304.
22 M. Nišavić, A. Hozić, Z. Hameršak, M. Radić, A. Butorac, M. Duvnjak and M. Cindrić, *Anal. Chem.*, 2017, **89**, 4847–4854.
23 J. Will, W. S. Sheldrick and D. Wolters, *JBIC J. Biol. Inorg. Chem.*, 2008, **13**, 421–434.
24 J. Will, A. Kyas, W. S. Sheldrick and D. Wolters, *JBIC J. Biol. Inorg. Chem.*, 2007, **12**, 883–894.
25 M. S. Wilm and M. Mann, *Int. J. Mass Spectrom. Ion Process.*, 1994, **136**, 167–180.
26 C. Artner, H. U. Holtkamp, W. Kandioller, C. G. Hartinger, S. M. Meier-Menches and B. K. Keppler, *Chem. Commun.*, 2017, **53**, 8002–8005.
27 F. Wang, A. Habtemariam, E. P. L. van der Geer, R. Fernández, M. Melchart, R. J. Deeth, R. Aird, S. Guichard, F. P. A. Fabbiani, P. Lozano-Casal, I. D. H. Oswald, D. I. Jodrell, S. Parsons and P. J. Sadler, *Proc. Natl. Acad. Sci. U. S. A.*, 2005, **102**, 18269–18274.
28 A. M. Pizarro, A. Habtemariam and P. J. Sadler, in *Medicinal Organometallic Chemistry*, eds. G. Jaouen and N. Metzler-Nolte, Springer Berlin Heidelberg, 2010, pp. 21–56.
29 M. Nišavić, M. Stoiljković, I. Crnolatac, M. Milošević, A. Rilak and R. Masnikosa, *Arab. J. Chem.*, , DOI:10.1016/j.arabjc.2016.07.021.
30 S. Cosconati, S. Forli, A. L. Perryman, R. Harris, D. S. Goodsell and A. J. Olson, *Expert Opin. Drug Discov.*, 2010, **5**, 597–607.
31 J. Lu, A. J. Stewart, P. J. Sadler, T. J. T. Pinheiro and C. A. Blindauer, *Biochem. Soc. Trans.*, 2008, **36**, 1317–1321.
32 W. Bal, M. Sokołowska, E. Kurowska and P. Faller, *Biochim. Biophys. Acta*, 2013, **1830**, 5444–5455.
33 I. Moraleja, E. Moreno-Gordaliza, D. Esteban-Fernández, M. L. Mena, M. W. Linscheid and M. M. Gómez-Gómez, *Anal. Bioanal. Chem.*, 2015, **407**, 2393–2403.
34 G. Ferraro, L. Massai, L. Messori and A. Merlino, *Chem. Commun.*, 2015, **51**, 9436–9439.
35 A. Merlino, *Coord. Chem. Rev.*, 2016, **326**, 111–134.
36 A. Levina, J. B. Aitken, Y. Y. Gwee, Z. J. Lim, M. Liu, A. M. Singharay, P. F. Wong and P. A. Lay, *Chem. – Eur. J.*, 2013, **19**, 3609–3619.
37 D. Chatterjee, A. Mitra, A. Levina and P. A. Lay, *Chem. Commun. Camb. Engl.*, 2008, 2864–2866.
38 W. H. Ang, A. Casini, G. Sava and P. J. Dyson, *J. Organomet. Chem.*, 2011, **696**, 989–998.
39 W. Hu, Q. Luo, X. Ma, K. Wu, J. Liu, Y. Chen, S. Xiong, J. Wang, P. J. Sadler and F. Wang, *Chem. Weinh. Bergstr. Ger.*, 2009, **15**, 6586–6594.
40 A. R. Timerbaev, C. G. Hartinger, S. S. Aleksenko and B. K. Keppler, *Chem. Rev.*, 2006, **106**, 2224–2248.

View Article Online
DOI: 10.1039/C7MT00330G

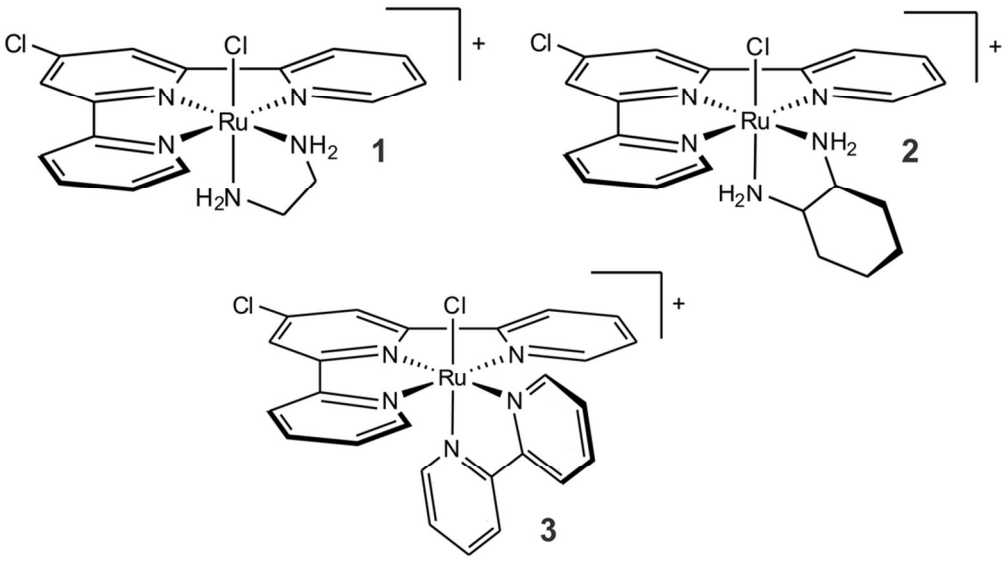

Figure 1.

46x25mm (600 x 600 DPI)

View Article Online
DOI: 10.1039/C7MT00330G

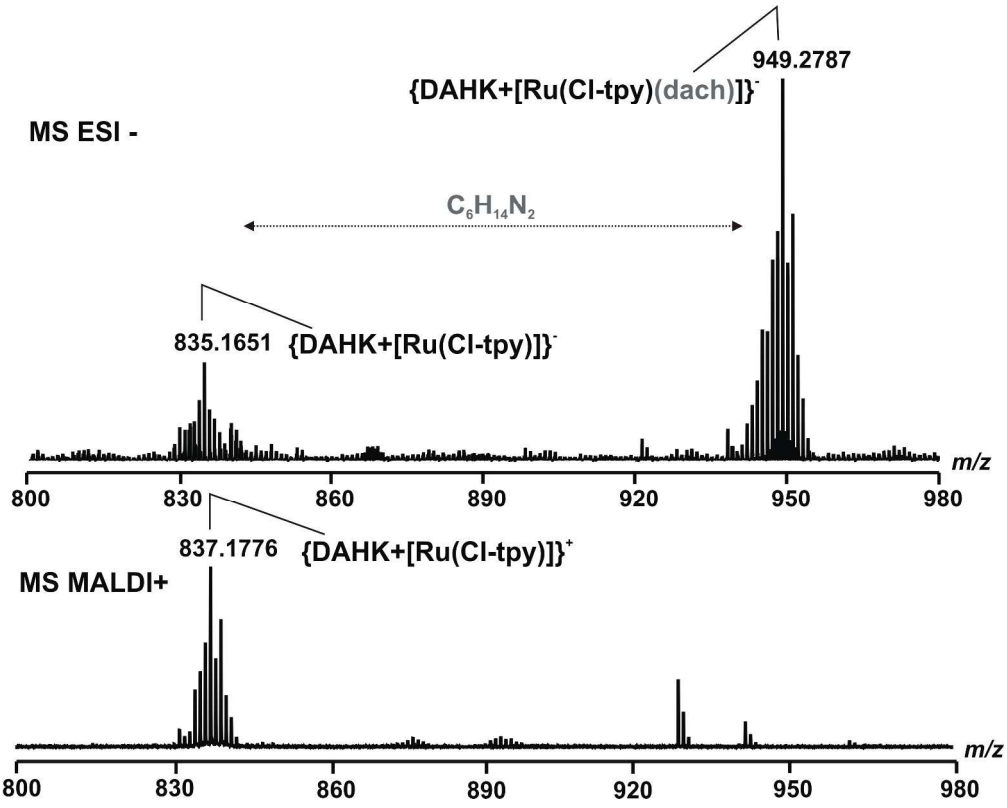

Figure 2.

View Article Online
DOI: 10.1039/C7MT00330G

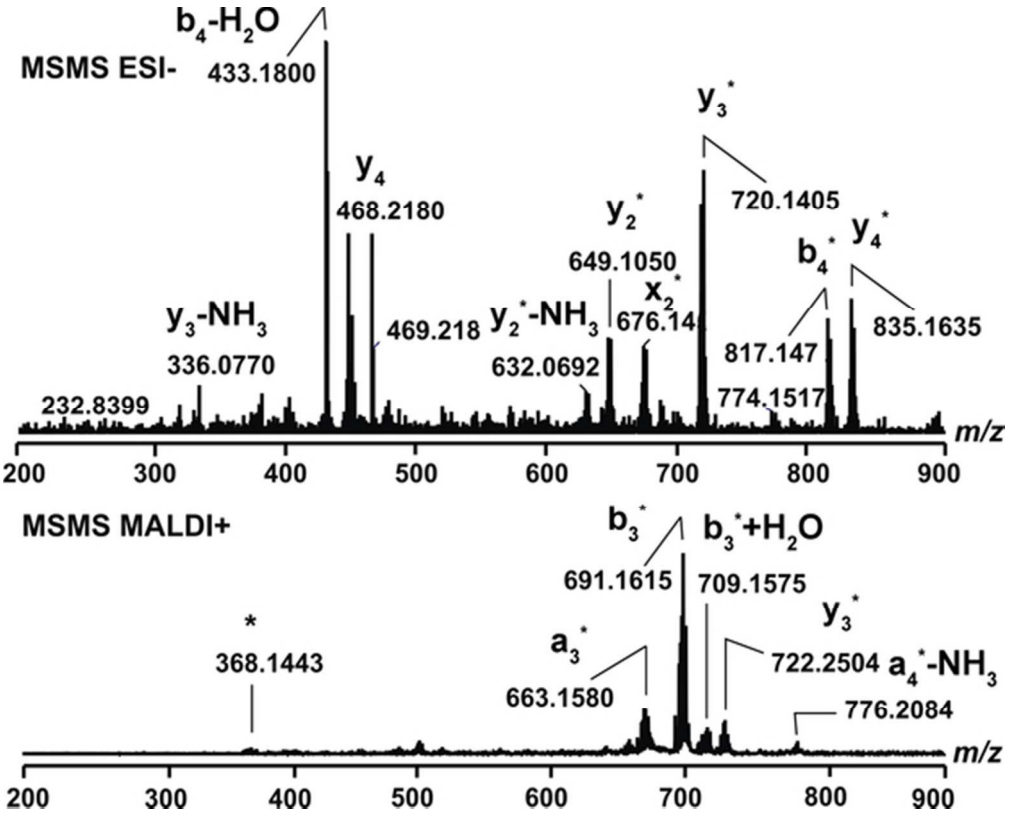

Figure 3.

26x20mm (600 x 600 DPI)

View Article Online
DOI: 10.1039/C7MT00330G

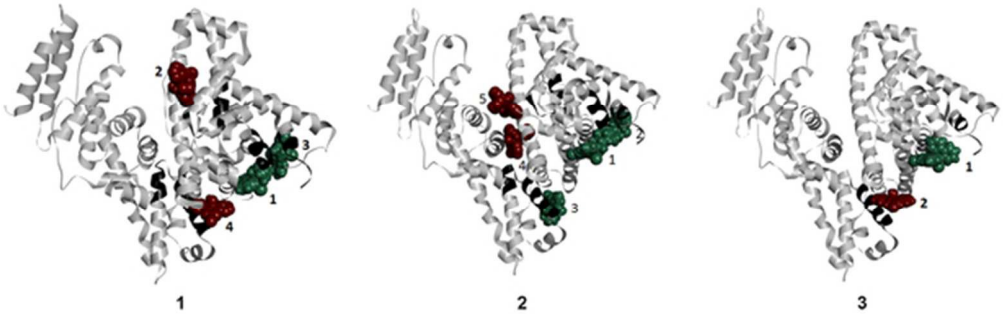

Figure 4.

25x8mm (600 x 600 DPI)

View Article Online
DOI: 10.1039/C7MT00330G

Table 1. Binding energies and target amino acids for coordination of investigated Ru(II) complexes **1**, **2** and **3** on HSA.

Binding site	Binding energy (kcal/mol)		
	1	**2**	**3**
1	**-8,12** [RuCl(4'-Cl-tpy)(en)]$^+$ *His67, His3*	**-9,14** [RuCl(4'-Cl-tpy)(dach)]$^+$ *His67, His3*	**-6,98** [RuCl(4'-Cl-tpy)(bipy)]$^+$ *His9,His3,His67*
2	**-7.80** [RuOH(4'-Cl-py)(en)]$^+$ *His146*	**-8,38** [RuOH(4'-Cl-tpy)(dach)]$^+$ *His9*	**-5,84** [RuOH(4'-Cl-tpy)(bipy)]$^+$ *Asp324*
3	**-7,09** [RuCl(4'-Cl-tpy)(en)]$^+$ *His338*	**-8,37** [RuOH(4'-Cl-tpy)(dach)]$^+$ *Asp324*	-
4	**-6,83** [RuCl(4'-Cl-tpy)(en)]$^+$ *His9*	**-6,48** [RuOH(4'-Cl-tpy)(dach)]$^+$ *His338*	-
5	**-5,84** [RuOH(4'-Cl-tpy)(en)]$^+$ Asp324	**-6,47** [RuOH(4'-Cl-tpy)(dach)]$^+$ *His146*	-